Source Correlated Prompt Neutron Activation Analysis for Material Identification and Localization

Bonnie Canion, Seth McConchie, and Sheldon Landsberger

***Abstract*— This paper investigates the energy spectrum of photon signatures from an associated particle imaging deuterium tritium (API-DT) neutron generator interrogating shielded uranium. The goal is to investigate if signatures within the energy spectrum could be used to indirectly characterize shielded uranium when the neutron signature is attenuated. By utilizing the correlated neutron cone associated with each pixel of the API-DT neutron generator, certain materials can be identified and located via source correlated spectrometry of prompt neutron activation gamma rays. An investigation is done to determine if fission neutrons induce a significant enough signature within the prompt neutron-induced gamma-ray energy spectrum in shielding material to be useful for indirect nuclear material characterization. The signature deriving from the induced fission neutrons interacting with the shielding material was slightly elevated in polyethylene-shielding depleted uranium (DU), but was more evident in some characteristic peaks from the aluminum shielding surrounding DU.**

***Index Terms*— Radiation detectors.**

I. Introduction

THIS paper investigates the gamma rays that are induced by 14-MeV deuterium tritium (DT) source neutrons, correlated in time and direction to the source neutron by the associated particle imaging (API) method, and detected by a gamma spectrometry detector.

The goal is to investigate if any signatures related to fission interactions in uranium appear in the photon energy spectrum for low-Z shielded uranium. For a low-Z shielding material, such as polyethylene, the neutron signatures are potentially attenuated too greatly to be usable for analysis. This is particularly true for fast neutron detection, which typically cannot detect fission neutrons after a single scatter with hydrogenous material due to high detector thresholds. However, gamma rays travel through low-Z material with low rates of attenuation. If the neutrons released from a fission chain would induce inelastic scattering gamma rays that show up in the energy spectrum, the signature could potentially be used to indirectly identify and characterize highly shielded uranium. The interaction cross section is small for fission energy neutrons' inelastic scattering in many materials so the noise has to be low, which is why the API technique is employed.

In this investigation, the shielding materials investigated are polyethylene and aluminum. Polyethylene is of interest because it is an effective neutron moderator, and the carbon has a relevant characteristic gamma ray induced from the first excitation of the (n, n') interaction. Aluminum is a less effective neutron moderator, but it has several prompt neutron-induced characteristic gamma rays, providing more opportunity to look for signs of fission neutron-induced signature.

In order to investigate this potential signature, it is first necessary to demonstrate the ability of this API prompt gamma spectrometry technique to identify materials in a narrow field of view, such that there is low interference from the surrounding material. This is important because carbon and aluminum are common elements, and it is necessary to prove that the signature is from the inspection object, instead of surrounding materials. The chain of events that needs to occur for this signature has a low probability of occurring, meaning that we are looking for a weak signature, and the ability to precisely separate out the desired signature from background is necessary.

After understanding this technique's ability to focus on an inspection object, it is then necessary to observe the source correlated gamma-ray signature that is detected from shielded uranium. However, since the source neutrons also induce gamma rays within the shielding material, it is necessary to separate out the signature induced from just the fission neutrons. Measurements comparing shielded depleted uranium (DU) and a matching configuration of shielded tungsten were analyzed to look for evidence of fission neutron-induced characteristic gamma rays. Since tungsten has a similarly high density as uranium, it serves as a nonfissioning surrogate material.

II. Theory

The physical mechanism behind this technique is to bombard a material with fast neutrons, which excite the nuclei via various interactions and cause the release of gamma rays with energies that are characteristic of the nuclear structure of the isotope. The detection of these characteristic gamma rays can then be used for material identification. Different techniques utilize different types of neutron interactions, which

Manuscript received July 1, 2016; revised December 7, 2016; accepted February 9, 2017. Date of publication March 6, 2017; date of current version July 14, 2017. This work was supported in part by the U.S. Department of Homeland Security under Grant 2012-DN-130-NF0001-02 and in part by the U.S. Department of Energy, National Nuclear Security Administration under Contract DE-AC52-07NA27344.

B. Canion is with the Lawrence Livermore National Laboratory, Livermore, CA 94550 USA (e-mail: canion1@llnl.gov).

S. McConchie is with the Oak Ridge National Laboratory, Oak Ridge, TN 37831 USA (e-mail: mcconchiesm@ornl.gov).

S. Landsberger is with the University of Texas at Austin, Austin, TX 78712 USA (e-mail: s.landsberger@mail.utexas.edu).

Color versions of one or more of the figures in this paper are available online at http://ieeexplore.ieee.org.

Digital Object Identifier 10.1109/TNS.2017.2678523

dictates the neutron energy and the detection time frame used. Since this research focuses on the API technique with 14-MeV neutrons, only gamma rays that reach the detector within a small time window of the source particle detection (tens of nanoseconds) will be included in the final gamma-ray energy spectrum, which primarily limits the relevant interactions to inelastic scattering.

The nature of the technique requires gamma rays from interactions with high cross sections and/or high energy characteristic gamma rays, since the low interaction probability and geometric efficiency lead to low detection rates of relevant gamma rays. These qualifications limit the materials that can be identified using this technique. A good resource for gamma-ray energies and cross sections induced by 14-MeV neutrons for various isotopes can be found in the International Nuclear Data Committee (INDC) report [1].

For carbon, the 14.1-MeV inelastic scattering macroscopic cross section in polyethylene is about 0.009 cm^{-1} [1], [2]. Since fission neutrons span an energy range and several neutrons are released per fission, the probability per centimeter of polyethylene per fission interaction that an inelastic scattering gamma ray will be produced in carbon is

$$P_C = M\nu \sum_{E=4.8}^{10} \Sigma_E^{n,n'} P_E^n \tag{1}$$

where ν is the average number of neutrons produced from a 14.1-MeV-induced fission, M is the fission chain multiplication, and the summation is equal to the inelastic cross section for polyethylene weighted by the probability of a fission neutron being produced at that energy, over the relevant energy range (P_E^n is calculated via a Watt spectrum). Plugging in cross-sectional data from ENDF [2], this value ends up being about 0.003 cm^{-1} per fission for DU shielded by polyethylene.

For the DU casting used in these measurements, the probability of the 14.1-MeV neutron inducing a fission is roughly 18%. There will be significant differences in the transport of the source neutrons through the inspection object compared to the fission neutrons through the shielding material. However, based on these cross-sectional values, it is expected that a couple of percent of the gamma rays seen in the characteristic carbon peak will have been induced by fission neutrons.

III. Relevant Literature

The use of a DT neutron generator for active interrogation followed by prompt gamma-ray spectrometry to identify unknown materials for security applications has been done by a few groups, usually for nondestructively identifying materials in explosives [3]–[5]. In many instances, the gamma rays are not correlated with a source, but are collected over the whole measurement time [6], [7]. Other groups utilize the timing characteristics of the source to inform the gamma-ray energy spectrum; for example, the pulsed fast/thermal neutron analysis technique uses a pulsed generator to collect gamma rays from inelastic scattering when the neutron pulse is on, and prompt gamma rays from absorption of neutrons when the pulse is off [6].

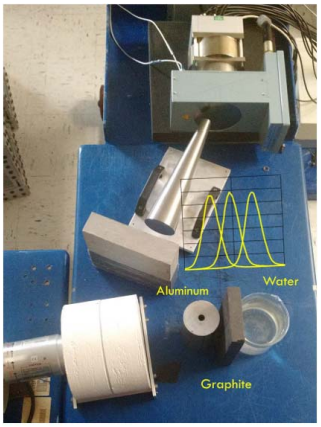

Fig. 1. Experimental setup of measurement done to determine the ability of this technique to differentiate nearby materials.

The advantages of using the API method for prompt gamma-ray spectrometry are the high level of background suppression and the ability to localize the signatures emitted from a specific field of view. Particularly for common elements (e.g., carbon, oxygen, and aluminum), the ability to use the spatial and timing information to separate out the gamma rays derived from the inspection object, as opposed to surrounding materials, is very advantageous. The disadvantage of using API-DT generators for this technique is the limitations in the maximum neutron flux for these systems compared to other portable neutron generators, leading to potentially longer measurement times.

The three main systems in the open literature that use an API-DT generator to generate source correlated prompt gamma-ray spectra for material identification purposes are EURITRACK, UNCOSS, and SENNA. EURITRACK [8], [9] was designed to investigate large cargo containers; UNCOSS [10] was designed for underwater explosives detection; and SENNA [11] was designed for boxes and luggage. Based on the open literature, all the three systems were built for nondestructive explosives detection, though EURITRACK also performed some investigations with nuclear material [4]. Therefore, the previous work differs from the work presented here, which focuses on combinations of nuclear material with shielding material and differentiating nearby materials on a finer scale.

IV. Experimental Setup

The API-DT neutron generator used for these measurements is a VNIIA ING-27 generator with a continuous flux rated to go up to 10^8 neutrons/s. Owing to limitations on personnel dosimetry in the laboratory space, the generator was run at a maximum of around 10^7 neutrons/s. This model of neutron generator has a built-in segmented Si alpha detector. The segmented detector is a line of 15 pixels, each 6×6 mm^2 in size. [12]

The HPGe detector used was an Ortec Gamma-X N-type coaxial "pop-top" model detector cooled by liquid nitrogen. The signal from the detector anode was run directly into a CAEN 5724 4 channel 14-bit 100-MS/s digitizer, and collected using the CAEN pulse height analysis control software (DPP-PHA).

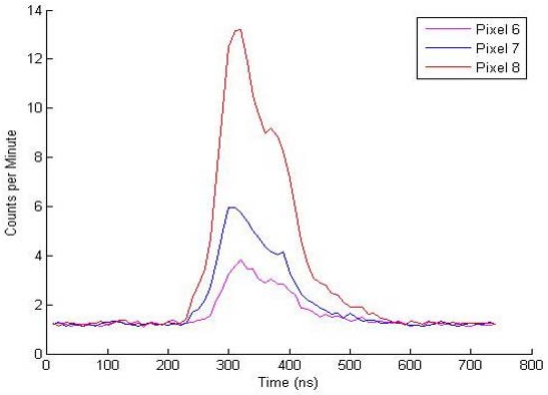

Fig. 2. Correlation of the induced radiation detected in the HPGe detector following a detection in the specified alpha pixel. The pulse magnitude decreases from one pixel to the next primarily due to self-attenuation in the object, such that gamma rays induced in the object that are correlated with pixel 6 need to travel through much of the inspection object to reach the detector.

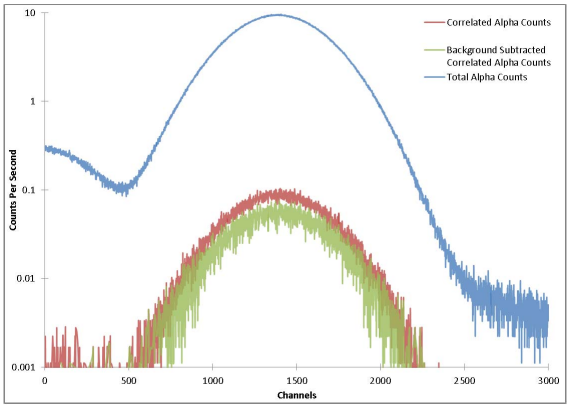

Fig. 3. Pulse height spectra of the total alpha counts, alpha counts correlated with the HPGe detector, and correlated alpha counts with background subtracted.

The signals from alpha pixels 6, 7, and 8 were input into three of the digitizer channels, along with the HPGe signal. Target objects were placed about 55 cm away from the front of the generator, with the detector placed to the side. The HPGe detector had a tungsten cone 30.5 cm long and lead bricks between the generator and the Ge crystal to shield the crystal from the source neutrons. There was also a lead shield that surrounded the Ge crystal for additional shielding. With this level of shielding, it was determined that the detector damage from the DT generator would be insignificant.[1] The setup can be seen in Fig. 1.

The field of view of the pixels of the alpha detector is plotted and placed onto the experimental setup image in Fig. 1 to illustrate the orientation of the correlated neutron cones. The three pixels used for these measurements span about a 20 horizontal field of view. All the targets were placed within this field of view. The DPP-PHA CAEN software converts the pulses into triangular waveforms based on the user inputs. The pulse height of the triangular waveform is proportional to the energy deposited in the detectors and is recorded for spectrometry. The data were output in list mode, which included all timing and pulse height information for events that exceeded a user defined threshold. A post-processing program determined the correlations between the alpha pixel source pulses and the HPGe-induced radiation pulses based on the timing information. The user can define a correlation time window, which defines the region of the true correlated-induced radiation.

In order to determine an appropriate correlation window, a correlation plot is created to show the rate of gamma rays detected in time bins relative to the time of the source event. Fig. 2 shows the peak from the induced radiation following the source event for each alpha pixel. The true signature is estimated to be from 220 to 590 ns based on the plot in Fig. 2.[2]

Fig. 3 shows the pulse height spectrum of the alpha pulse. This pulse height spectrum is not useful for the analysis because the alpha pulses serve only as a trigger, but is shown here to illustrate how this technique essentially removes accidental correlations from the spectra. The top blue line shows the pulse height distributions of all the alpha pulses for the uncorrelated pixels recorded during this 30-min measurement. The main peak corresponds to true alpha pulses (around channels 475 up to 2500), while the lower energy tail corresponds to electronic noise and X-rays that are not correlated with a source event.

When looking at the correlated alpha counts (red line in Fig. 3), it is immediately obvious that the total number of correlated alpha pulses is a small percentage of the total number of alpha pulses. There is a low probability that a source 14-MeV neutron will create prompt gamma rays in the target object, which make it into the small detector crystal and then deposit enough energy to exceed the threshold. Therefore, this severe reduction in alpha counts is understandable.

Note that in the red line in Fig. 3, there are still some low pulse height counts in the correlation plot that are not true alpha pulses. This implies that there is a small rate of accidental correlations. This is not very surprising when looking back at Fig. 2 and noticing the background rate of around 1.5 counts/min/ns after the source event. In order to subtract out this background contribution, a correlation window of the same size is taken in a background region of the correlation plot (starting at 1 μs), and the pulse height spectrum from this region is subtracted from the correlated pulse height spectrum.

The results of this process are shown in Fig. 3 by the green plot. In this background subtracted spectrum, it appears

[1]In these initial measurements, the HPGe detector was about 65 cm away from the source, which reduces the flux reaching the 7 cm diameter and 9-cm-long detector crystal to around 0.1% of the total flux based on a solid angle. The shielding of a 30-cm cone of tungsten and an additional 10 cm of lead further reduces the source neutron flux to around 0.06% of the original flux reaching the crystal, based on an MCNP calculation. This leads to a negligible level of source neutrons reaching the detector crystal. Neutrons originating from the inspection object will be lower energy neutrons than the source neutrons, so the damage level will be less severe. This is a low enough dose rate to the crystal so that detector damage will be a significant problem for these purposes.

[2]The absolute difference in time between the source event and the beginning of this peak does not represent the time-of-flight in this case, because it includes differences in the cable lengths and pulse processing and detector properties. The time-of-flight information was not needed for this analysis.

TABLE I
ENERGIES OF SOME OF THE PROMPT GAMMA RAYS THAT ARE LIKELY TO BE SEEN IN SPECTRA FROM THESE MEASUREMENTS

Energy (keV)	Element
803	Pb
834	Ge
844	Al
847	Fe
931	Fe
1014	Al
1095	Pb
1238	Fe
1590	Pb
1720	Al
1770	Pb
1809	Al
2211	Al
2615	Pb
3004	Al
4439	C
6130	O

that the accidental correlation rate is essentially nonexistent, meaning that the spectrum will be made up of true correlated prompt radiation, though much of it is still true correlated background. It is clear that this method is an excellent way to reduce the background, in spite of the significantly reduced count rate.

V. MEASUREMENTS

A. Characterizing the Capabilities of the Experimental Setup

Before investigating the main signature of interest, it is necessary to establish the following.

1) The signatures in the correlated spectra are from the target object alone, and not from the surrounding material.
2) The shielding material signatures can easily be detected in a reasonable amount of time.
3) Enriched uranium would not add a significant background to the spectra to interfere with the characteristic gamma-ray signatures.

1) Identification and Localization of Material: The first goal is to verify that this setup could be used to identify characteristic gamma rays above the background and in a specified region without significant contributions from adjacent materials. A different material was put into the field of view of each pixel side by side to see how well this technique could be used to identify and differentiate these objects. As shown in Fig. 1, an aluminum annular cylinder was placed in the view of pixel 8, a graphite brick was placed in front of pixel 7, and a container of water was in view of pixel 6. For all the measurements, the DT neutron generator continuously outputs between 9×10^6 and 1×10^7 neutrons/s. A measurement was taken for 60 min. Table I gives the characteristic gamma rays of some materials present in this section.

The results of the measurement are shown in Fig. 4. In the total spectrum, shown in black, it is clear that a variety of materials are present; contributions from all the three target objects are clear. There is also evidence of the lead shielding (2.62 MeV) and iron in structural materials (1.24 and 0.85 MeV), even though these materials are not prevalent in the target object. Aluminum is present, but it could be from either the table or the inspection object (3.00 MeV).

By correlating the HPGe detector to each alpha pixel, it is clear which material is in the field of view. The spectrum correlated with pixel 8 is shown in green, which was aimed at the aluminum target. The aluminum peaks are easy to identify, and are the strongest signatures (besides the large 511 keV peak). The blue spectrum is correlated with pixel 7, which was aimed at graphite. The resolution of the carbon peak (4.44 MeV) is noticeably worse than the other peaks,[3] making the peak not as clear, but definitively above background, along with the first escape peak (3.93 MeV). The red spectrum correlated with pixel 6, which was aimed at the container of water, is the most difficult to see. This is due to both the attenuation from the other two objects and the low efficiency of HPGe, especially for high-energy photons. Despite this, it is still possible to identify the 6.13-MeV-gamma-ray peak from oxygen, as well as its first escape peak at 5.62 MeV.

It is very impressive how well the nearby objects are filtered out of these pixel correlated spectra. Although the objects are right next to each other, and the pixel views overlap slightly, it is very clear what the predominant material associated with each pixel is. The contribution from the adjacent materials in the spectra is hardly even discernible. The downside of this technique, again, is the very low count rates in the relevant source correlated energy peaks. The best way to combat this problem would be to add additional HPGe detectors to the setup or increase the source neutron rate.

2) Time to Detect: Given the large reduction in total counts when using this method, the amount of time required for a measurement could be a concern. For this technique to be useful, the relevant peaks must be detectable within a few minutes to a few hours, depending on the application. A summary of the previous measurement is shown in Table II. In this table, the integrals of the peaks of interest for each material are given for both the correlated and total spectra, along with the uncertainty information, in units of counts per minute (CPM). Spectra from the background time region were subtracted from each integral, and included in the uncertainty determination. The peak to background (BG) ratio is also given for each gamma-ray energy peak, which is the counts in the highest count channel divided by the average of the background on either side of the peak. Using the count rates and background rates for each gamma-ray peak, the amount of time required for the counts to exceed the detection limits, as defined in [13], was determined.

The results in Table II highlight the strengths and weaknesses of utilizing the peaks from the source correlated spectra versus those in the total spectra. The BG ratios are significantly higher for the source correlated spectra, which makes sense considering how effective this method is at reducing the background. Comparing the count rates, the time to detectability is always significantly shorter for the peaks in the total spectrum

[3]It is important to note that the poor resolution of the carbon peak compared to the rest of the peaks present is due to a physical phenomenon particular to the carbon nuclear interaction; when the carbon nucleus is excited, the decay time is so short that the nucleus is still recovering from the collision, which leads to Doppler broadening of the energy peak.

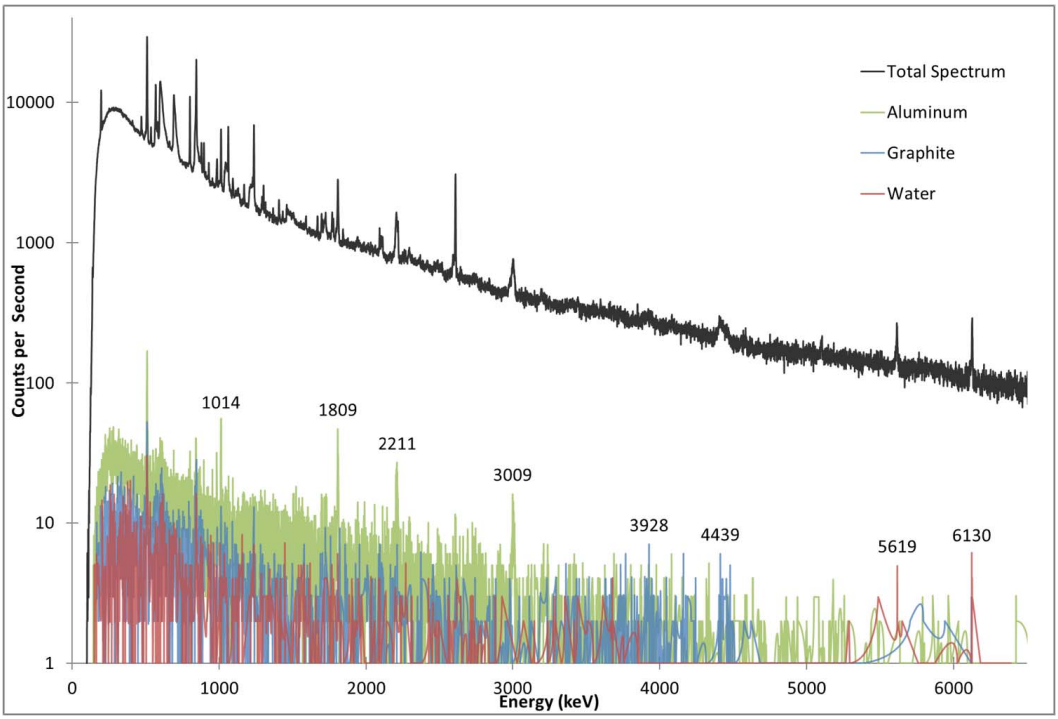

Fig. 4. Correlated and total spectra of the measurement shown in Fig. 1.

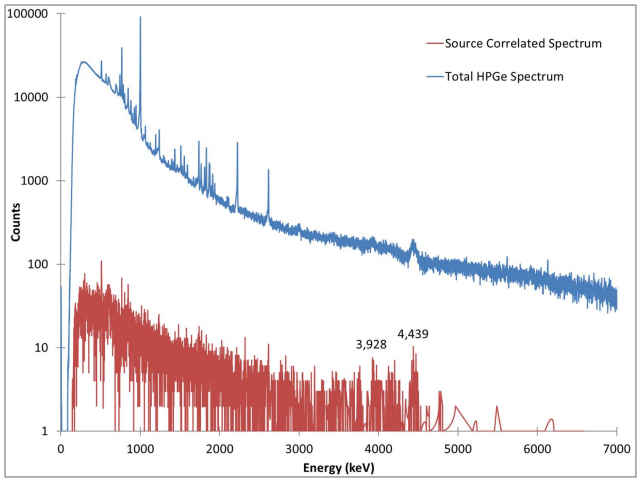

Fig. 5. Correlated and total spectra of polyethylene-shielded DU.

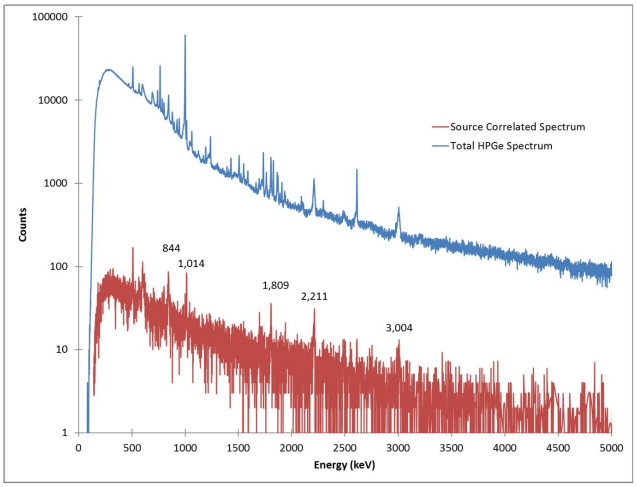

Fig. 6. Correlated and total spectra of aluminum-shielded DU.

due to the higher counting statistics. However, many of the peaks in the source correlation method are still detectable in less than 10 min. The oxygen peaks in water were the most difficult of those studied. However, it is important to remember that the field of view was small (around 3), and the attenuation high for that measurement.

Again, the main benefit of the source correlation method is not quantifiable in Table II, which is that the nonrelevant peaks drop out of the spectra, making it easier to determine what isotopes are present in the target object.

3) Investigating Signatures From Shielded Uranium: Now that it has been well established that the correlated spectra are effectively seeing the target material and not adjacent materials, the signature from the uranium shielded by polyethylene and aluminum is investigated. Each measurement of the DU casting surrounded by 5 cm of shielding was taken for 30 min. The results plotted in Figs. 5 and 6 include the total spectrum taken by the HPGe detector during each 30-min measurement, as well as the source-correlated HPGe spectrum. Again, by excluding all data outside of the correlation window, the count rates drop dramatically. For these particular spectra, the main carbon peak (4.4 MeV) and its escape peaks will be the signatures that identify the presence of the polyethylene-shielding material. The hydrogen present in the polyethylene does not have a prompt activation signature. The strong presence of the 2.22-MeV peak in the total spectrum is due

TABLE II
INTEGRALS OF THE PEAKS OF INTEREST FROM SPECTRA SHOWN IN FIG. 4

Energy (MeV)	CPM	Peak to BG Ratio	Time Until Detectable (min)	CPM	Peak to BG Ratio	Time Until Detectable (min)
	Source Correlated Spectra			*Total Spectra*		
Pixel 8 - Aluminum (Figure 4)						
1.81	4.4 ± 0.4	9.00	3.7	233.6 ± 4.4	2.65	0.2
2.21	4.2 ± 0.4	6.44	3.3	NA - Hydrogen interference		
3.00	2.9 ± 0.3	8.06	5.7	107/8 ± 3.7	1.69	0.7
Pixel 7 - Graphite (Figure 4)						
3.93	1.1 ± 0.3	6.48	48.0	34.1 ± 4.7	1.24	12.3
4.44	2.6 ± 0.3	12.18	5.6	83.5 ± 4.2	1.51	1.6
Pixel 6 - Water (Figure 4)						
5.61	0.3 ± 0.1	12.86	73.1	20.6 ± 1.5	1.97	3.0
6.13	0.5 ± 0.1	19.64	22.4	23.1 ± 1.4	2.59	2.1

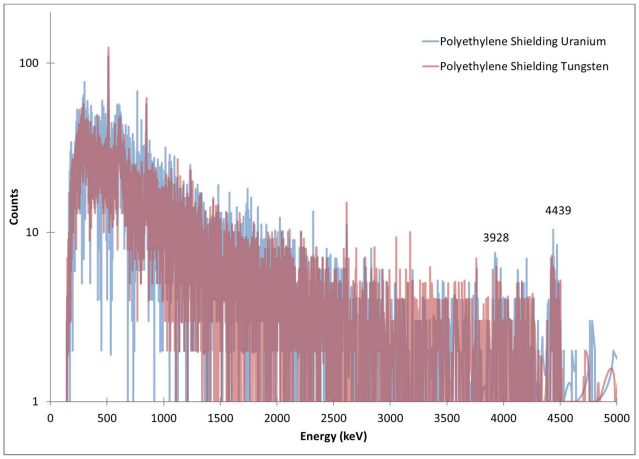

Fig. 7. Comparing polyethylene-shielding DU with tungsten to search for fission-induced signatures.

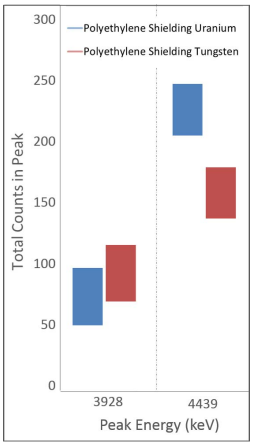

Fig. 8. Comparison of the integrals of carbon peaks, seen in Fig. 7.

primarily to thermalized neutron interactions with hydrogen, but these gamma rays are not present in the prompt time region. However, the 4.44-MeV peak from carbon and its first escape peak at 3.93 MeV are present in both the total and correlated spectra in Fig. 5.

For the aluminum-shielded DU, there are several characteristic gamma rays labeled in Fig. 6, which are the strongest among the many aluminum characteristic gamma rays. Again, they unambiguously show the presence of aluminum in the correlated neutron region, which has few other peaks.

Again, various elements are evident in the total spectrum, but the most prevalent signature of the correlated spectra are the relevant characteristic gamma rays in the target object.

4) Simulations of Varying Enrichment: Simulations were performed in MCNP PoliMi [14] as an exploration of how uranium signatures vary with enrichment. This is an effect that we cannot look at experimentally, due to lack of access to enriched uranium. The same 18-kg annular casting of uranium used in these measurements was compared to an enriched uranium version of the same geometry. The results are not shown for brevity, but can be seen in [15]. The main difference between the two was the abundance of low-energy photons, which makes sense due to the increased fission activity in the enriched uranium casting. Given the low geometric efficiency of the HPGe detector, this increased number of photons is unlikely to overwhelm the detector experimentally. However, it is important to consider that gamma-ray peaks will likely have a reduced signal to BR below around 3 MeV.

B. Investigation of Signature Induced From Fission

It has been established that this technique can be used to specify a target and that polyethylene and aluminum-shielding DU can be identified by the characteristic peaks, all in a timely manner. Now the contribution of the signature from the fission neutrons will be investigated.

Two measurements of each shielding type were performed for 20 min each: the DU casting with shielding and the tungsten casting with shielding. This was done to see if the characteristic peaks are different between the shielded DU and tungsten, which each have similar levels of gamma-ray attenuation. If the characteristic peak is larger on the shielded DU spectrum compared to shielded tungsten, it could signify fission neutrons activating the shielding material in a detectable way.

VI. RESULTS

The resulting spectra are shown in Fig. 7 for polyethylene and Fig. 9 for aluminum. Comparing the carbon peaks of the shielded uranium and tungsten in Fig. 7, it is not possible to visually determine a difference in the number of counts; the 4.44 and the 3.93 MeV peaks both appear to be comparable.

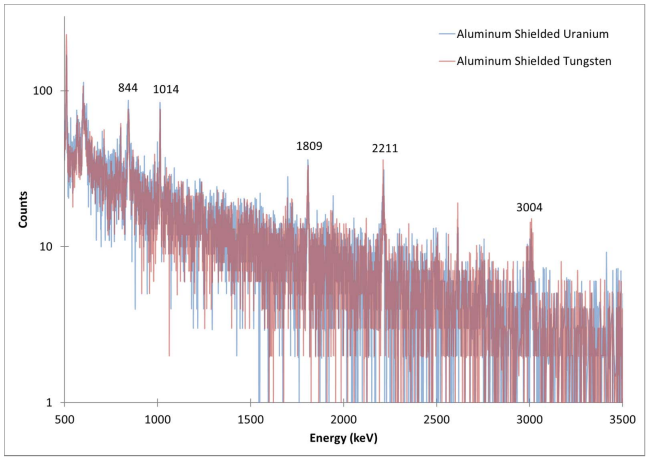

Fig. 9. Comparing aluminum-shielding DU with tungsten to search for fission-induced signatures.

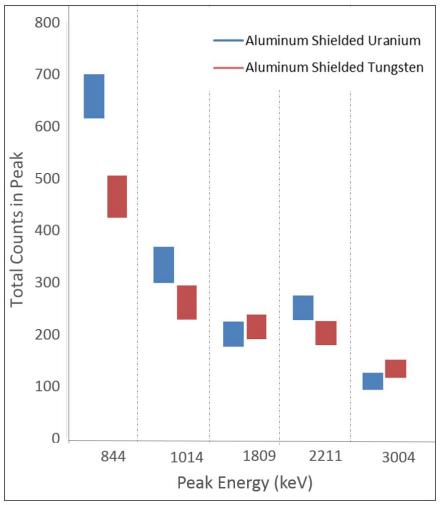

Fig. 10. Comparison of the integrals of aluminum peaks, seen in Fig. 9.

Integrating both peaks for each inspection object, the 4.44 MeV peak builds at a rate of 7.5 ± 0.7 cpm for uranium and 5.3 ± 0.7 cpm for tungsten. The first escape peak builds at a 2.4 ± 0.8 cpm for uranium and 3.1 ± 0.8 cpm for tungsten. The range of total counts is visually represented in Fig. 8. The 4.4 peak is higher for uranium than tungsten in a statistically significant way, though by a small margin. The escape peaks are comparable. The difference between the shielded uranium and tungsten 4.4-MeV peaks is interesting, but not very convincing and actually the same within 5 sigma. However, considering that the contribution from the fission neutron-induced signature is expected to be at most a few percent of the total counts, this could be what is causing the difference between the two.

The polyethylene is an interesting shielding material to investigate primarily because it is an effective neutron moderator, so a technique that could provide an indirect signature would be useful. Aluminum is primarily interesting because it is also a relatively low-Z material and has multiple characteristic gamma rays to investigate. The strongest characteristic gamma rays are labeled in Fig. 9, and the results of the range of total counts is summarized in Fig. 10.

Based on the significant difference between the lowest energy characteristic gamma ray of 844 keV, there is a strong enough difference between the results from the uranium and tungsten that there are likely significant characteristic gamma rays being produced by fission neutrons. The fact that the difference between the characteristic gamma rays in the uranium and tungsten objects decreases as the gamma ray energy increases makes sense because the fission neutrons are less likely to have enough energy to induce a significant rate of excitations.

VII. Conclusion

The explorations leading up to looking for this fission signature gave positive results, showing the usefulness of source-correlated prompt gamma-ray spectrometry toward the goal of identifying and localizing material. The positive results are in line with previous research that has been done by other groups, as discussed previously. However, many of the previous studies focused on bulk items, correlating larger pixel segments to much larger target objects such as shipping containers, as opposed to differentiating adjacent smaller target objects.

This paper was primarily focused on building confidence in the ability of this technique to localize and identify material in a target object in a timely manner, and determine whether or not a significant fission neutron-induced signature could be seen.

The results from this series of measurements show that we are most likely seeing characteristic gamma rays induced by fission neutrons for lower energy characteristic gamma-ray peaks, which can be induced by a greater portion of the fission-energy neutron spectrum. It is possible, but not conclusive, that there were contributions from the fission neutrons in the characteristic carbon peak. It is much more likely that the significant difference in the 844-keV-characteristic aluminum peak contained fission neutron-induced gamma rays. The results suggest that the signature is significantly stronger for characteristic gamma rays below 1 MeV. However, low-energy noise may begin to degrade the quality of the spectrum for higher enrichment uranium targets, particularly as increases in gamma rays directly from fission would also scale up with increasing enrichment.

Future studies could adjust source neutron rate, detection efficiency, and correlation time window in order to see a stronger fission neutron-induced signature. Since multiple neutrons are released from a single-source-correlated fission chain, an interesting investigation could be to look for correlated fission-neutron-induced characteristic gamma rays, though the detector efficiency would likely need to be increased significantly.

Acknowledgment

The authors would like to thank C. Tintori from CAEN for lending his digitizer expertise and software. The views and conclusions contained in this document are those of the authors and should not be interpreted as necessarily representing the official policies, either expressed or implied, of the U.S. Department of Homeland Security.

REFERENCES

[1] S. P. Simakov, A. Pavlik, H. Vonach, and S. Hlaváč, "Status of experimental and evaluated discrete γ-ray production at E_n=14.5 MeV," IAEA, Vienna, Austria, Tech. Rep. INDC(CCP)-413, 1998.

[2] *Evaluated Nuclear Data Files (ENDF)*, accessed on Nov. 2015. [Online]. Available: https://www-nds.iaea.org/endf

[3] E. Rhodes, C. E. Dickerman, T. Brunner, A. Hess, and S. Tylinski, "APSTNG: Associated particle sealed-tube neutron generator studies for arms control," Argonne Nat. Lab., Lemont, IL, USA, Tech. Rep. ANL/ACTV-95/1, 1994.

[4] B. Pérot *et al.*, "Materials characterisation with the associated particle technique," in *Proc. IEEE Nucl. Sci. Symp. Med. Imag. Conf. (NSS/MIC)*, Anaheim, CA, USA, Oct. 2012, pp. 1702–1711.

[5] D. S. Koltick, "The integrated detection of hazardous materials," in *Proc. AIP Conf.*, vol. 680. 2003, pp. 835–839.

[6] A. P. Barzilov, I. S. Novikov, and P. C. Womble, "Material analysis using characteristic gamma rays induced by neutrons," in *Gamma Radiation*. InTech, 2009, pp. 4–5.

[7] A. L. Swift, B. R. Grogan, J. A. Mullens, J. P. Hayward, and J. T. Mihalczo, "Attributes from NMIS time coincidence, fast-neutron imaging, fission mapping, and gamma-ray spectrometry data," in *Proc. Inst. Nucl. Mater. Manage. Conf.*, Orlando, FL, USA, 2012, pp. 15–19.

[8] B. Pérot, G. Perret, and A. Mariani, "The EURITRACK project: Status of a tagged neutron inspection system for cargo containers," *Proc. Tech. Meeting Padova*, pp. 1–5, Nov. 2007.

[9] W. El Kanawati *et al.*, "Acquisition of prompt gamma-ray spectra induced by 14 MeV neutrons and comparison with Monte Carlo simulations," *Appl. Radiat. Isot.*, vol. 69, no. 5, pp. 732–743, May 2011.

[10] C. Carasco *et al.*, "Data acquisition and analysis of the UNCOSS underwater explosive neutron sensor," *IEEE Trans. Nucl. Sci.*, vol. 59, no. 4, pp. 1438–1442, Aug. 2012.

[11] D. N. Vakhtin, I. Y. Gorshkov, A. V. Evsenin, A. V. Kuznetsov, and O. I. Osetrov, "Senna—Portable sensor for explosives detection based on nanosecond neutron analysis," in *Detection and Disposal of Improvised Explosives* (NATO Security Through Science Series), H. Schubert and A. Kuznetsov, Eds. Dordrecht, The Netherlands: Springer, 2006.

[12] "Neutron generators for elemental analysis of substances and materials," All Russia Res. Inst. Autom., Moscow, Russia, Tech. Rep. [Online]. Available: http://www.vniia.ru/eng/ng/element.html

[13] L. A. Currie, "Limits for qualitative detection and quantitative determination: Application to radiochemistry," *Anal. Chem.*, vol. 40, no. 3, pp. 586–593, Mar. 1968.

[14] S. A. Pozzi *et al.*, "MCNPX-PoliMi for nuclear nonproliferation applications," *Nucl. Instrum. Methods Phys. Res. A, Accel. Spectrom. Detect. Assoc. Equip.*, vol. 694, pp. 119–125, Dec. 2012.

[15] B. E. Canion, "Incorporation of photon analysis into an active interrogation system for shielded uranium characterization," Ph.D. dissertation, Dept. Mech. Eng., Univ. Texas, Austin, TX, USA, 2016.